

SEMICLASSICAL TRANSPORT PROPERTIES AND SHELL STRUCTURE IN THE NUCLEAR COLLECTIVE DYNAMICS

A. G. Magner, A. M. Gzhebinsky, S. N. Fedotkin

Institute for Nuclear Research, National Academy of Sciences of Ukraine, Kyiv, Ukraine

For the low-lying collective excitations in nuclei the transport coefficients are derived within the periodic orbit theory at the lowest orders of semiclassical expansion corresponding to the extended Thomas - Fermi approach. The multipole surface vibrations near the spherical shape are described within the time-dependent mean field approximated through the infinitely deep square-well potential. It is shown that the smooth collective inertia is essentially larger than that of irrotational flow due to the consistency condition for density and potential. The smooth transport coefficients are used as a macroscopic background in the modified shell correction method for the description of slow nuclear collective dynamics. After this renormalization, the quantum cranking model formula for inertia becomes in agreement with the semiclassical results at large particle numbers and temperatures. The collective vibration energies, reduced friction and effective damping coefficient are in better agreement with experimental data than those found from the hydrodynamic model.

1. Introduction

For calculations of the static nuclear properties like the total binding and deformation energy, the famous shell correction method (SCM) was suggested by Strutinsky [1] and successfully applied in many further works, see for instance [2, 3]. The nuclear energy was defined in [1] as a sum of the phenomenological macroscopic part given by the liquid-drop energy and the shell correction. The SCM is based on the concept of existence of the quasiparticle spectrum near the Fermi surface by the Migdal theory of finite fermion systems with a strong interaction of the particles [4]. Within this concept, the shell component of free energy can be considered perturbatively as a quasiparticle correction to the total nuclear free energy on basis of the statistically averaged (macroscopic) background described phenomenologically through the liquid drop model or the extended Thomas - Fermi (TF) approach [3].

In order to extend these ideas to the collective dynamics for the description of low-energy nuclear excitations [4 - 6], the simple proposals were suggested in [7, 8] by employing the response theory. The collective variables were introduced there explicitly as deformation parameters of a mean single-particle field. The nuclear excitations were parametrized in terms of the transport coefficients, such as the stiffness, the inertia and the friction parameters defined through the adequate collective response functions. In analogy with the SCM, the response function was split into the smooth macroscopic and the fluctuative shell components. Its fluctuative part was calculated semiclassically within the Periodic Orbit Theory (POT) [3, 9 - 11], which is a powerful analytical tool for study of the shell effects in level densities and energy shell corrections.

The main purpose of this work is more specific suggestion of simpler version of the SCM splitting with applying it immediately to the transport coefficients for slow collective motion. The averaged transport coefficients can be simplified analytically with help of the POT at the lowest orders in \hbar , which correspond to the extended TF approximation. With the consistency condition between the particle density and the potential variations [6, 12], this TF approach can be useful as a macroscopic background in the formulation of the Strutinsky SCM.

For the energy dissipation rate, a simple macroscopic derivation of the famous wall formula for the friction due to collisions of particles of the perfect Fermi-gas with a slowly moving surface of the mean-field potential well was suggested in [13]. From a quite general classical (Thomas - Fermi) and quantum starting point, Koonin and Randrup have rederived this wall formula for the average friction with smooth trajectory components in [14]. For the quantum case, the multiple reflection expansion of Green function by Balian and Bloch [15], which is based on the iteration procedure with the zero approximation for free particle motion, was used in [14, 16, 17]. Other independent derivations of the wall formula with focus on specific averaging procedures can be found e.g. in [18, 19]. The SCM averaging procedure and Thomas - Fermi approach for level density were applied in [19] for relating the wall formula to the averaged quantum friction coefficient.

In the present paper we derive the explicit analytical expressions for friction and inertia by the method based on the Gutzwiller path-integral version of the POT [3, 9, 11] at leading orders in \hbar . In Section 2, we begin with a general response function formalism following basically [6]. For the infinitely deep spherical square-well potential, in Section 3 we obtain the semiclassical friction and inertia parameters in close relation with the approach of [14, 16 - 18] for the friction case. The smooth semiclassical collective transport

coefficients, which satisfy the consistency condition, and the corresponding multipole vibration energies, the reduced and effective friction coefficients are derived and compared with experimental data [20 - 22] in Section 4. In Section 5, we try to extend the SCM to the transport coefficient calculations for slow collective motion by using the consistent TF approximation for the macroscopic background. Our SCM results for the temperature dependences of the quadrupole vibration energies, the reduced and effective friction parameters are compared in Section 6 with their counterparts of the quantum cranking model [6, 19] as well as with experimental data cited in [23 - 25]. The conclusion remarks are discussed in Section 7.

2. Response Theory and Transport Coefficients

Many-body collective excitations are conveniently described in terms of the nuclear response to an external perturbation, $V_{\text{ext}} = \hat{F}q_{\omega}^{\text{ext}} e^{-i\omega t}$, where q_{ω}^{ext} is a vibration amplitude, and \hat{F} some one-body operator. Its quantal average, $\langle \hat{F} \rangle_t$, at time t can be calculated through the Fourier transform, $\langle \hat{F} \rangle_{\omega}$, obtained within the linear response theory [5, 6]

$$\langle \hat{F} \rangle_{\omega} = -\chi_{FF}^{\text{coll}}(\omega)q_{\omega}^{\text{ext}}, \quad \hat{F} = \left(\frac{\partial V}{\partial Q} \right)_{Q=Q^{(0)}}, \quad (1)$$

where $\chi_{FF}^{\text{coll}}(\omega)$ is the collective response function. (Here and in the following we assume vanishing unperturbed average value $\langle \hat{F} \rangle^{(0)}$). The nuclear Hamiltonian at $q_{\omega}^{\text{ext}} = 0$ depends on a collective variable Q as the time-dependent deformation parameter of mean field potential $V(Q)$ in Eq. (1), $Q^{(0)}$ is a static deformation. For the axially symmetric multipole vibrations of the nuclear surface with the radius $R(\theta, Q)$ near the spherical shape, in the spherical coordinates r, θ, φ one writes $R(\theta, Q) = R[1 + Q(t)Y_{L0}(\theta)]$, $Q(t) = Q_{\omega} e^{-i\omega t}$. (The unperturbed quantities are indeed zero in this case, $Q^{(0)} = 0$ and $\langle \hat{F} \rangle^{(0)} = 0$). With the consistency condition [6],

$$\langle \hat{F} \rangle_{\omega} = \kappa Q_{\omega}, \quad \kappa = -\chi(0) - C(0), \quad (2)$$

where κ is the coupling constant, $C(0)$ the stiffness, $C(0) = \left(\partial^2 \mathcal{F} / \partial Q^2 \right)_{Q=0}$, \mathcal{F} the nuclear free energy, $\chi(0)$ the isolated susceptibility, the collective response $\chi_{FF}^{\text{coll}}(\omega)$ can be expressed in terms of the so called ‘‘intrinsic’’ response function $\chi(\omega)$ [5, 6]. Assuming also one dominating separate peak in the strength function, $\text{Im}\chi_{FF}^{\text{coll}}(\omega)$, this relationship in the Q-mode can be conveniently written in an inverted form [6, 8, 12]:

$$\frac{1}{\chi_{QQ}^{\text{coll}}(\omega)} = \frac{1}{\chi_{QQ}(\omega)} + \kappa \approx -M\omega^2 - i\gamma\omega + C, \quad \chi_{QQ}(\omega) = \frac{\chi(\omega)}{\kappa^2} = -\frac{1}{\kappa^2} \frac{\langle \hat{F} \rangle_{\omega}}{Q_{\omega} + q_{\omega}^{\text{ext}}}. \quad (3)$$

Here, the inverse collective response function, $\chi_{QQ}^{\text{coll}}(\omega)$, for low frequencies is approximated by the corresponding response function of a damped harmonic oscillator with the stiffness C , the inertia M , and the friction γ parameters, as shown in Eqs. (3). Such self-consistent transport coefficients were related in [6, 12] to the auxiliary parameters $C(0)$, $\gamma(0) = -i[\partial\chi/\partial\omega]_{\omega=0}$ and $M(0) = [(1/2)\partial^2\chi/\partial\omega^2]_{\omega=0}$, as the coefficients of expansion of the ‘‘intrinsic’’ response function, $\chi(\omega)$, in ω in the ‘‘zero-frequency limit’’, $\omega \rightarrow 0$, for slow enough collective motion,

$$C = \left[1 + \frac{C(0)}{\chi(0)} \right] C(0), \quad \gamma = \left[1 + \frac{C(0)}{\chi(0)} \right]^2 \gamma(0), \quad M = \left[1 + \frac{C(0)}{\chi(0)} \right]^2 \left(M(0) + \frac{\gamma(0)^2}{\chi(0)} \right). \quad (4)$$

The ‘‘intrinsic’’ response $\chi(\omega)$, see Eqs. (3), can be expressed in terms of the one-body Green function G [7, 12, 17],

$$\chi(\omega) = \frac{2}{\pi} \int_0^{\infty} d\varepsilon n(\varepsilon) \int d\mathbf{r}_1 \int d\mathbf{r}_2 \hat{F}(\mathbf{r}_1) \hat{F}(\mathbf{r}_2) \text{Im} G(\mathbf{r}_1, \mathbf{r}_2, \varepsilon)$$

$$\times \left[G^*(\mathbf{r}_1, \mathbf{r}_2, \varepsilon - \hbar\omega) + G(\mathbf{r}_1, \mathbf{r}_2, \varepsilon + \hbar\omega) \right], \quad G = \sum_i \frac{|i\rangle\langle i|}{\varepsilon - \varepsilon_i + i\Gamma}, \quad (5)$$

where $n(\varepsilon)$ is the Fermi occupation numbers at the energy ε for temperature T , $n(\varepsilon) = \{1 + \exp[(\varepsilon - \lambda)/T]\}^{-1}$, λ the chemical potential. The factor 2 accounts for the spin degeneracy. For the Green function $G(\mathbf{r}_1, \mathbf{r}_2, \varepsilon)$ (the asterisk means the complex conjugation), we may use, see [42], the spectral representation of Eqs. (5) with eigenvalues ε_i , eigenfunctions $|i\rangle$, and $\Gamma \rightarrow +0$ in the mean field approximation. With Eqs. (5), the friction $\gamma(0)$ is zero and the inertia $M(0)$ of Eqs. (4) is equivalent to the cranking model inertia in this mean-field limit,

$$M = 2\hbar^2 \sum'_{ij} \frac{n_i - n_j}{(\varepsilon_j - \varepsilon_i)^3} |\langle i | \hat{F} | j \rangle|^2. \quad (6)$$

The prime means that the diagonal terms $\varepsilon_i = \varepsilon_j$ are excluded in the summations, see g.e. [6].

3. Semiclassical Approach

The ‘‘intrinsic’’ response function $\chi(\omega)$, Eqs. (5), can be found with help of the semiclassical expansion of Green function G derived by Gutzwiller [3, 9] from the quantum path-integral propagator

$$G(\mathbf{r}_1, \mathbf{r}_2, \varepsilon) = \sum_{\alpha} G_{\alpha}(\mathbf{r}_1, \mathbf{r}_2, \varepsilon) = -\frac{1}{2\pi\hbar^2} \sum_{\alpha} |\mathfrak{J}_{\alpha}(\mathbf{p}_1, t_{\alpha}; \mathbf{r}_2, \varepsilon)|^{1/2} \exp\left[\frac{i}{\hbar} S_{\alpha}(\mathbf{r}_1, \mathbf{r}_2, \varepsilon) - \frac{i\pi}{2} \mu_{\alpha}\right]. \quad (7)$$

The index α covers all classical paths inside the potential well, which connect the two spatial points \mathbf{r}_1 and \mathbf{r}_2 for a given energy ε , and S_{α} is the classical action along such trajectory α . The μ_{α} denotes the phase related to the Maslov index through the number of all caustic and turning points of the path α [3]. The oscillation amplitude in Eqs. (7) depends on the classical trajectory stability measured by the Jacobian, $\mathfrak{J}_{\alpha}(\mathbf{p}_1, t_{\alpha}; \mathbf{r}_2, \varepsilon)$, for transformation from the initial momentum \mathbf{p}_1 and time t_{α} of the particle motion along the trajectory α to its final coordinate \mathbf{r}_2 and energy ε . For closed orbits α , $\mathbf{r}_2 \rightarrow \mathbf{r}_1 = \mathbf{r}$, a continuous axial symmetry related to the existence of families of the periodic orbits crossing a given point \mathbf{r} in the spherical potential well has to be taken into account [11] in the semiclassical calculations of the oscillation amplitudes in Eqs. (7). For such a family, this amplitude of the Green function term, G_{α} , in expansion (7) over α , see Eqs. (16), (31) of [11], is enhanced by factor proportional to $\hbar^{-1/2}$ with respect to that in the case of the *isolated* trajectories given in the last equation of Eqs. (7).

Among all classical trajectories α , we may single out α_0 which connects directly \mathbf{r}_1 and \mathbf{r}_2 without reflections from the potential well edge. For the Green function G , Eqs. (7), one has then a separation, $G = G_{\alpha_0} + G_{osc}$, which leads to the corresponding splitting of the slightly averaged level density, $g(\varepsilon)$, into a smooth part of the Thomas - Fermi model, $g_{TF}(\varepsilon)$, and its shell structure correction, $g_{osc}(\varepsilon)$, $g(\varepsilon) = g_{TF}(\varepsilon) + g_{osc}(\varepsilon)$. We shall use more exact smooth density $g_{ETF}(\varepsilon)$ of the extended Thomas - Fermi model, with including the surface and curvature \hbar corrections instead of the volume part $g_{TF}(\varepsilon)$, see [3, 9 - 11]. The POT sum over the periodic orbits, $g_{osc}(\varepsilon)$, describes the shell effects in the single-particle spectrum.

For calculations of the semiclassical friction, $\gamma(0)$, and inertia, $M(0)$, one can substitute the trajectory expansion of Green function (7) into Eq. (5) for the response function $\chi(\omega)$ and take then its derivatives in ω at $\omega = 0$. Here, we have to deal with both closed ($\mathbf{r}_1 = \mathbf{r}_2$) and non-closed ($\mathbf{r}_1 \neq \mathbf{r}_2$) trajectories α , in contrast to the calculations of level density trace. For the integration over spatial coordinates \mathbf{r}_1 and \mathbf{r}_2 in

Eqs. (5), we specify now the coordinate dependence of the single-particle operator $\hat{F}(\mathbf{r})$, Eqs. (1), for the multipole vibrations of surface of the spherical square-well potential with the infinitely high walls,

$$\hat{F}(\mathbf{r}) = -V_0 R \delta(r - R) Y_{L_0}(\theta), \quad \frac{2m}{\hbar^2} V_0 G \rightarrow \left(\frac{\partial^2 G}{\partial r_1 \partial r_2} \right)_{r_j=R}, \quad j=1,2, \quad (8)$$

for $V_0 \rightarrow \infty$, where V_0 is the potential well depth, m the nucleon mass. With this expression for the operator \hat{F} and the boundary condition, Eqs. (8), the integrals over the spatial coordinates \mathbf{r}_1 and \mathbf{r}_2 in Eqs. (5) are reduced to the double surface integrals over a spherical cavity edge because of $\delta(r - R)$ in Eq. (8). Due to the azimuthal symmetry, the corresponding friction, $\gamma(0)$, and inertia, $M(0)$, are simplified furthermore, namely,

$$\gamma(0) = -i \left(\frac{\partial \chi(\omega)}{\partial \omega} \right)_{\omega=0} = \frac{8\pi \hbar^5 R^6}{m^2} \sum_{\alpha\alpha'} \int_0^\infty d\varepsilon n(\varepsilon) \int_0^\pi d\theta_1 \sin\theta_1 \int_0^\pi d\theta_2 \sin\theta_2 Y_{L_0}(\theta_1) Y_{L_0}(\theta_2) \times \\ \times \left(\frac{\partial^2 \text{Im} G_\alpha}{\partial r_1 \partial r_2} \frac{\partial}{\partial \varepsilon} \frac{\partial^2 \text{Im} G_{\alpha'}}{\partial r_1 \partial r_2} \right)_{r_j=R}, \quad (9)$$

$$M(0) = \frac{1}{2} \left(\frac{\partial^2 \chi(\omega)}{\partial \omega^2} \right)_{\omega=0} = \frac{4\pi \hbar^6 R^6}{m^2} \sum_{\alpha\alpha'} \int_0^\infty d\varepsilon n(\varepsilon) \int_0^\pi d\theta_1 \sin\theta_1 \int_0^\pi d\theta_2 \sin\theta_2 Y_{L_0}(\theta_1) Y_{L_0}(\theta_2) \times \\ \times \left[\frac{\partial^2 \text{Im} G_\alpha}{\partial r_1 \partial r_2} \frac{\partial^2}{\partial \varepsilon^2} \left(\frac{\partial^2 \text{Re} G_{\alpha'}}{\partial r_1 \partial r_2} \right) \right]_{r_j=R}. \quad (10)$$

We took into account the factor of 2 due to the time reversibility symmetry [11]. For the calculations of these friction and inertia coefficients, we need to study separately the two different cases:

- (i) the *nearly local* case, $S_\alpha(\mathbf{r}_1, \mathbf{r}_2, \varepsilon_F)/\hbar = k_F L_\alpha \lesssim 1$, $\varepsilon_F = \hbar^2 k_F^2 / 2m$ and
- (ii) *non-local* contributions, $k_F L_\alpha \gg 1$,

where L_α is the length of the trajectory α , k_F the Fermi momentum in units of \hbar .

In the case (i), after the Strutinsky averaging [1 - 3], the most important contribution is coming from the trajectory, $\alpha = \alpha' = \alpha_0$, with a *short* length, $L_{\alpha_0} = s = |\mathbf{r}_2 - \mathbf{r}_1| \lesssim 1/k_F \ll R$, for large semiclassical parameter, $k_F R \gg 1$. For simplicity of calculations of the contributions (i), $\alpha = \alpha' = \alpha_0$, into Eqs. (9) for the friction $\gamma(0)$, and (10) for the inertia $M(0)$, the variables $\{\theta_1, \theta_2\}$ can be transformed to $\{\zeta, \bar{x}\}$ through $\{x, \bar{x}\}$ by the two steps, $x = \cos\theta_2 - \cos\theta_1$, $\bar{x} = [\cos\theta_2 + \cos\theta_1]/2$ and $x = -\zeta^2/2y^2$, where $y = kR$, $\zeta = ks$, s is the length of the trajectory α_0 with the ends near the spherical boundary, $s \approx 2R \sin[(\theta_2 - \theta_1)/2]$. The Green function G_{α_0} from Eqs. (7) in the new variables $\{\zeta, \bar{x}\}$ for small enough length s of the trajectory α_0 , $s/R \ll 1$, is reduced approximately to a simple analytical form G_0 for free particle motion [26]

$$G_{\alpha_0}(\mathbf{r}_1, \mathbf{r}_2, \varepsilon) \approx G_0(\mathbf{r}_1, \mathbf{r}_2, \varepsilon) = -\frac{m}{2\pi \hbar^2 s} \exp(iks), \quad s = |\mathbf{r}_1 - \mathbf{r}_2|, \quad k = \sqrt{\frac{2m\varepsilon}{\hbar^2}}. \quad (11)$$

For calculation of the Jacobian \mathfrak{J}_α in Eqs. (7) we used transformation of the spatial and momentum variables to the cylindrical coordinates and then moving coordinate system in the α -trajectory plane with axes, perpendicular and parallel to the α , $\mathfrak{J}_\alpha \approx m^2 \cos\phi / 2aR^2 \sin\phi \sin\psi$, $\phi = (\psi + 2\pi b)/2a$, $\psi = \theta_2 - \theta_1$, a is the number of turning points for planar trajectory α [26]. We point out that the Gutzwiller trajectory expansion (7) differs essentially from the multiple-reflection one [15] used in [14, 16], even for the case of

potentials with a sharp edge like cavity (or box) potentials [26]. In contrast to G_0 of [15], the term G_{α_0} in expansion (7) for the case of spherical cavity has another pre-exponent Jacobian factor as function of the initial angle variables and depends on the Maslov index [3].

The integrals over angles θ_1 and θ_2 for the terms $\alpha = \alpha' = \alpha_0$ in Eqs. (9), (10) can be calculated analytically within the approximation (11). We integrated also over the energy ε by parts in order to transform the integrals to those with the integrands containing the sharp bell-like factor of $\partial n/\partial \varepsilon$ near the chemical potential, $\lambda \approx \varepsilon_F$, for small enough temperature, $T/\varepsilon_F \ll 1$. For such finite temperature, we may use expansion in the semiclassical parameter $1/kR$ near the Fermi surface $k \approx k_F$, then the Strutinsky averaging in kR (for the case of inertia) and the Sommerfeld expansion of smooth functions of the energy ε , as compared to the derivative $\partial n/\partial \varepsilon$, see g.e. [6]. The standard Strutinsky averaging [1, 2, 19]¹ was applied in order to remove all terms oscillating as functions of kR with the suitable Gaussian weight width Δ and correction polynomial of degree $2\mathcal{M}$ on the stability plateau. The averaging “width” Δ has to be large enough of the order of a few gross shells in the single-particle spectrum of $k_F R$ in the spherical cavity [1, 2, 11, 19]. Note that in the case (ii) the contributions of longer trajectories, in particular, other non-diagonal ($\alpha \neq \alpha'$) components of the Green function expansion (7), were suppressed exponentially with increasing both the trajectory length, L_α , and the SCM averaging parameter, Δ , in kR variable at $k \approx k_F$, like in the POT level density calculations [3, 11]. Thus, for the quadrupole vibrations at leading orders in $k_F R$, we arrive finally at the following *nearly local* results for the semiclassical (TF) friction $\gamma_{\text{TF}}(0)$ and inertia $M_{\text{TF}}(0)$ [26]

$$\gamma_{\text{TF}}(0) = \gamma_{\text{wf}} \left(1 + \gamma_{\text{cor}}\right) \left(1 + \frac{\pi^2 \bar{T}^2}{3}\right), \quad \gamma_{\text{wf}} = \frac{\hbar (k_F R)^4}{4\pi^2}, \quad \gamma_{\text{cor}} = -\frac{1}{42}, \quad (12)$$

$$M_{\text{TF}}(0) = \frac{mR^2}{8\pi} \left[\frac{16(k_F R)^3}{385\pi} \left(1 + \frac{\pi^2 \bar{T}^2}{8}\right) - (k_F R)^2 + \frac{87368 k_F R}{9009\pi} \left(1 - \frac{\pi^2 \bar{T}^2}{24}\right) \right], \quad \bar{T} = \frac{T}{\varepsilon_F}. \quad (13)$$

The friction $\gamma_{\text{TF}}(0)$ (12) coincides approximately ($\bar{T} \ll 1$) with the wall formula γ_{wf} obtained earlier in [13, 14, 18, 19] in the *local* approximation $\mathbf{r}_1 \approx \mathbf{r}_2$ of the case (i), see g.e. Eq. (3.19b) in [14]. The temperature corrections in Eq. (12) was derived in [16]. A small correction γ_{cor} is related to the *non-local* terms of the order of $(s/R)^2$ in normal derivatives of $G_0(\mathbf{r}_1, \mathbf{r}_2, \varepsilon)$, see Eqs. (9) and (10) with the approximation (11). The inertia $M_{\text{TF}}(0)$, Eq. (13), in the limit $k_F R \rightarrow \infty$ is the sum of the leading “volume” term, $\propto (k_F R)^3$, the “surface” one, $\propto (k_F R)^2$, and the “curvature” correction, $\propto k_F R$ (besides of a common dimensional factor mR^2), similarly to the extended Thomas - Fermi expansion for the relationship of $k_F R$ to the particle number A

$$A = 2 \int_0^\infty d\varepsilon g_{\text{ETF}}(\varepsilon) = \frac{4(k_F R)^3}{9\pi} \left(1 + \frac{\pi^2 \bar{T}^2}{8}\right) - \frac{(k_F R)^2}{2} + \frac{4k_F R}{3\pi} \left(1 - \frac{\pi^2 \bar{T}^2}{24}\right), \quad (14)$$

with the extended TF level density $g_{\text{ETF}}(\varepsilon)$ [3,10]. (The factor of 2 accounts for the spin degeneracy and the weak \bar{T}^2 temperature dependence was found by the Sommerfeld expansion like in the derivation of Eqs. (12) and (13)). Therefore, we may call Eq. (13) for the inertia, and similarly, Eq. (12) for the friction, as the extended Thomas - Fermi (TF) approximation. Up to all *non-local* corrections in the integrand of Eqs. (10), (11) for $M(0)$, which are coming from small terms of the order of $(s/R)^2$ in the normal derivatives of G_0

¹ The averaging function, $f_{\text{av}}^{(2\mathcal{M})}((y - y')/\Delta)$, $y = kR$, $y' = k'R$ in spectrum y' , is defined by $f_{\text{av}}^{(2\mathcal{M})}(z) = e^{-z^2} P_{2\mathcal{M}}(z)/\sqrt{\pi}$, where $P_{2\mathcal{M}}(z) = \sum_{l=0,2,\dots}^{2\mathcal{M}} \alpha_l H_l(z)$ is the correction polynomial, $\alpha_l = -\alpha_{l-2}/2l$, $\alpha_0 = 1$, $H_l(z)$ is the Hermitian polynomial.

like in derivation of the local wall formula, the averaged inertia, $M_{\text{TF}}(0)$, coincides with a negative “surface” term of Eq. (13). As seen from Eq. (13), these *non-local* corrections can be even more important than the local ones for large enough $k_F R$ while the local term of the friction $\gamma_{\text{TF}}(0)$ (12) (wall formula) is always dominating at large $k_F R$.

Note that the other (non-local) smooth contributions (ii) of longer classical trajectories, $\alpha \neq \alpha_0$, into Eqs. (4.17) of [14] might be alternatively rederived from Eqs. (9) for $\gamma(0)$ and (10) for $M(0)$ by using the Gutzwiller expansion (7). In order to keep the leading terms in \hbar , we took into account that the derivatives of the strong oscillating exponent in G_α , Eqs. (7), are a factor $1/\hbar$ larger than those of the smooth amplitudes of G_α . The usual canonical relations of classical mechanics were used, too. With these leading terms, at large enough Gaussian averaging parameter Δ , which removes all oscillating terms, the only coherent diagonal ($\alpha = \alpha'$) components survive in Eqs. (9), (10). As noted in [14], the sums of these diagonal components over α are divergent, for instance, for the inertia, even after a renormalization procedure suggested there. However, as shown in [7] with help of the Gutzwiller approach [9] extended to continuous symmetries [11], the diagonal terms, $\alpha = \alpha'$, do not contribute into the *shell* components of the response function $\chi(\omega)$ (5), and hence, into Eqs. (9) for the friction and (10) for the inertia. These components are related to the *shell structure* part $\delta n(\varepsilon)$ of the occupation number $n(\varepsilon)$, $n = \tilde{n} + \delta n$ [1, 2, 7, 8]. After the Strutinsky averaging in the case (ii), the other (smooth) term $\tilde{n}(\varepsilon)$ in Eqs. (9) and (10) does not contribute also at the leading order in $k_F R$. Therefore, we are left with the nearly local approximation (12) and (13) for a smooth friction and inertia at the same order (without smooth trajectory components).

For evaluation of the contributions (ii) of longer trajectories, the Gutzwiller expansion (7) which contains the amplitudes valid for the *isolated* trajectories, fails because we have to account for a *continuous symmetry* of the spherical Hamiltonian (see the comment after Eq. (7)), i.e. for appearance of the axially-symmetric degenerated families of planar periodic orbits with a fixed vertex at the reflection boundary [11]. For the non-diagonal ($\alpha \neq \alpha'$) (ii) components of the angle integrals in Eqs. (9) and (10), according to the stationary-phase conditions, the leading terms in semiclassical parameter $k_F R$ are namely these *periodic orbits* [7, 8]. The non-diagonal ($\alpha \neq \alpha'$) terms of Eqs. (9) and (10) provide mainly the shell (non-local) corrections to the friction, $\gamma(0)$, and the inertia, $M(0)$, for smaller averaging parameter Δ through such periodic-orbit conditions. They will be discussed in details in further publications.

Notice, the temperature corrections in the friction for the Fermi gas system are proportional to T^2 like for the particles' rarely collisional (zero sound) regime in the Fermi liquids [6, 16, 19, 27, 28]. It is in contrast to its typical decreasing hydrodynamical behavior, $\propto 1/T^2$, due to the two-body viscosity of Fermi liquids in the case of the frequent collisions of particles. Similar small positive $(T/\varepsilon_F)^2$ corrections were obtained also in the TF inertia $M_{\text{TF}}(0)$ (13) while the irrotational flow inertia, $M_{\text{irr}} = 3mR^2 A/4\pi L$, is independent of temperature.

It should be noted that the only second (“surface”) term in the inertia, $M_{\text{TF}}(0)$ (13), and the wall formula, γ_{wf} in Eqs. (12), do not depend on the surface vibration multipolarity L . Other terms in Eqs. (12), (13) are presented for the quadrupole case $L = 2$.

In the macroscopic limit², $k_F R \rightarrow \infty$ (with averaging mentioned above), the only “volume” term of the inertia $M_{\text{TF}}(0)$ (13), that is proportional to $mR^2(k_F R)^3 \propto mR^2 A$, survives like the hydrodynamical inertia of irrotational flow, $M_{\text{irr}} \propto mR^2 A$, but having much smaller coefficient. For not too large semiclassical parameter, $k_F R \sim 10$, this “volume” term is smaller than the “surface” one by the absolute value. Therefore, their sum $M_{\text{TF}}(0)$ (“intrinsic” or inconsistent mass parameter, including the curvature term) is negative for these $k_F R$, see also [6]. We are going to show in the next section that the final result for the collective inertia

²The macroscopic approach is defined as the semiclassical limit $k_F R \rightarrow \infty$ after the *statistical averaging* in spectrum of kR with large enough Δ , which removes all oscillating terms like shell effects. This approach, similar to the extended TF, is *nearly local* approximation. Such averaging in kR ensures also a convergence of the semiclassical expansion in $1/kR$ (or \hbar) near the Fermi surface, $k \approx k_F$.

obtained from Eqs. (4) with help of the auxiliary “intrinsic” quantity $M_{\text{TF}}(0)$ (13) for $M(0)$ and *consistency condition* (2) is certainly positive, in accordance with positive values of the collective kinetic energy [6, 12].

4. Collective Transport Coefficients and Consistency

The smooth collective friction γ , which takes into account the consistency relation (2), can be obtained through Eqs. (4) with help of $\gamma_{\text{TF}}(0)$ (12) originating from the “intrinsic” response function $\chi(\omega)$. As known from [6, 12], for realistic nuclear parameters, the collective friction correction is determined by a small ratio, $C(0)/\chi(0) \approx -C(0)/\kappa$, with $C(0)$ and κ being the stiffness and coupling coefficients of the consistency condition (2). For their smooth values at the leading order of expansion in $A^{-1/3}$ within the effective nuclear surface approximation (ENSA) [29, 30] of the liquid drop model (LDM) [5, 30] one has

$$C_{\text{LD}} = \frac{b_s}{4\pi r_0^2} (L-1)(L+2) R^2, \quad \kappa_{\text{LD}} = -\frac{8b_v K R^4}{225\pi b_s r_0^4}. \quad (15)$$

Here, b_v the binding energy per nucleon, b_s is the surface energy constant, $r_0 = (3/4\pi\rho)^{1/3}$, ρ the particle density, $\rho = k_F^3/3\pi^2$, and K the incompressibility modulus of the infinite nuclear matter, $L \geq 2$. Notice, the ENSA relates the statistical TF approach to the LDM, based both on the description in terms of the local quantities, such as the particle, current and energy densities, the pressures and so on [29, 30]. For large particle numbers we have to add also the Coulomb term to the surface component of the LDM stiffness C_{LD} , Eqs. (15), along the β -stability line [5, 31]. With the conventional phenomenological values [33, 34], $\rho = 0.16 \text{ fm}^{-3}$ ($r_0 = 1.14 \text{ fm}$), $b_v = 16 \text{ MeV}$, $b_s = 18 \text{ MeV}$, $K = 220 \text{ MeV}$ (the symmetry coefficient $b_{\text{sym}} = 60 \text{ MeV}$), for the quadrupole ($L=2$) dimensionless ratio $C_{\text{LD}}(0)/\kappa_{\text{LD}}$, from Eqs. (15) one mainly finds a *small* quantity, $|C_{\text{LD}}(0)/\kappa_{\text{LD}}| \approx 2.6 A^{-2/3} \approx 0.2 \div 0.1$, at large enough particle numbers, $A = 40 \div 300$, respectively. For octupole case ($L=3$) one has $6.5 A^{-2/3}$ of the same order of smallness at larger particle numbers, $A = 150 \div 300$. Therefore, for *smooth* collective friction and stiffness at such particle numbers, one can set approximately $\gamma \approx \gamma_{\text{TF}}(0)$ and $C \approx C_{\text{LD}}$ in Eqs. (4).

However, it is not the case for the collective consistent inertia M defined by Eqs. (4). For this inertia at leading orders in $k_F R$, up to small temperature corrections, $\sim (T/\varepsilon_F)^2$, one obtains

$$M_{\text{TF}} = \left(1 + \frac{C_{\text{LD}}}{\chi_{\text{LD}}}\right)^2 (M_{\text{TF}}(0) + M_1), \quad M_1 = \frac{\gamma_{\text{TF}}(0)^2}{\chi_{\text{LD}}(0)} \approx -\frac{\gamma_{\text{wf}}^2}{\kappa_{\text{LD}}} = \frac{225mR^2 (k_F r_0)^4 b_s \varepsilon_F (k_F R)^2}{64\pi^3 b_v K}. \quad (16)$$

Here, $M_{\text{TF}}(0)$ is the “intrinsic” inertia (13), see also Eqs. (12), (15), (2), $\chi_{\text{LD}}(0) = -\kappa_{\text{LD}} - C_{\text{LD}}$. We may neglect the small ratio $C_{\text{LD}}/\kappa_{\text{LD}}$ in these equations. For simplicity, the small non-local friction correction γ_{cor} , Eqs. (12), was omitted in Eqs. (16), and the term M_1 becomes independent of the vibration multipolarity L , unlike the irrotational flow inertia M_{irr} .

For realistic nuclear parameters, $k_F R \sim 10$, the collective consistent component M_1 of the total inertia M_{TF} , Eqs. (16) is dominating above its “intrinsic” part, $M_{\text{TF}}(0)$, in the absolute value, $|M_{\text{TF}}(0)/M_1| = 0.04 \div 0.05$ for particle numbers $A = 40 \div 300$ related to $k_F R = 8 \div 14$, according to Eq. (14). It should be noted that this component M_1 , Eqs. (16), is smaller in order of $k_F R$ (or particle number parameter $A^{1/3}$) than the hydrodynamical inertia M_{irr} ,

$$\frac{M_1}{M_{\text{irr}}} = \frac{75(k_F r_0)^6 b_s \varepsilon_F L}{16\pi^2 b_v K A^{1/3}} \approx \frac{7.2L}{A^{1/3}} \quad (17)$$

($R = r_0 A^{1/3}$). However in fact, the inertia M_1 is larger essentially than M_{irr} due to a difference in coefficients. Indeed, one has the ratio, $M_1/M_{\text{irr}} \approx 4.2 \div 2.2$ for the quadrupole ($L=2$) and $6.3 \div 3.2$ for the

octupole ($L=3$) modes at particle numbers $A=40 \div 300$, respectively. Notice, with the “surface” and “curvature” corrections in the extended TF relationship, Eqs. (14), this ratio becomes even somewhat larger, $M_1/M_{\text{irr}}=5.6 \div 2.6$ for $L=2$ and $8.5 \div 3.8$ at $L=3$.

For smooth low-lying collective vibration energy

$$\hbar\omega_L = \hbar\sqrt{\frac{C}{M}} = \frac{D_L}{A^{1/3}}, \quad (18)$$

one finds a simple estimation:

$$D_L = \frac{8\pi\sqrt{(L-1)(L+2)}b_v K}{15\sqrt{2}(k_F r_0)^4} \approx 5\sqrt{(L-1)(L+2)} \text{ MeV}. \quad (19)$$

We derived these equations with help of the last equation in Eqs. (16) for the inertia, $M_{\text{TF}} \approx M_1$, and Eqs. (15) for the LDM stiffness C_{LD} . The nuclear parameters mentioned above were used on very right of Eqs. (19). Accounting for the “surface” and the “curvature” corrections of Eqs. (14) and collective $C_{\text{LD}}/\kappa_{\text{LD}}$ contributions in Eqs. (18), (4), (16) one has smaller values of D_L , which grow slowly with increasing particle number A , namely, $D_2 = 7 \div 9$ MeV and $D_3 = 12 \div 14$ MeV for $A = 40 \div 300$.

Fig. 1 shows the comparison of smooth TF dependences, Eqs. (18) and (19), $\propto A^{-1/3}$, at zero temperature with the experimental data for the low-lying quadrupole, $\hbar\omega_{2+}$ [20] (top), and octupole, $\hbar\omega_{3-}$ [21] (bottom), vibration energies [22]. The almost spherical nuclei with the quadrupole deformations $\beta_2 \sim < 0.01$ (quadrupole static deformations $Q^{(0)}$ in our denotation) are selected for the experimental data shown in this Figure [22, 32, 35 - 37]. The TF results (thin frequent dashed) are significantly improved with respect to the hydrodynamic (HD, rare dots) behavior, $\propto A^{-1/2}$. The reason of better agreement can be explained by larger TF inertias M_{TF} , Eqs. (16), than that of the irrotational flow, M_{irr} , see Eqs. (17), for enough heavy nuclei.

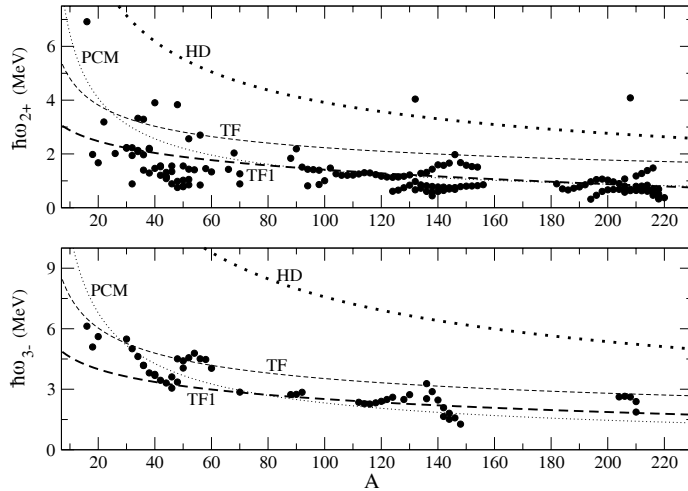


Fig. 1. Low-lying quadrupole $\hbar\omega_{2+}$ (top) and octupole $\hbar\omega_{3-}$ (bottom) vibration energies versus particle number A ; TF is given by Eqs. (18), (19); TF1 denotes this TF approach accounting for the Coulomb stiffness component [31, 5] and the surface corrections, as explained in the text; HD shows the standard LDM [5]. PCM (dotted) is $30A^{-2/3}$ MeV for $L=2$ (top) and $50A^{-2/3}$ MeV for $L=3$ (bottom) from [37]. Heavy full dots are the experimental data [22, 20, 21] for nearly spherical (even-even) nuclei with quadrupole deformations $\beta_2 < 0.05$ [22, 35, 36, 37]; $\rho = 0.16 \text{ fm}^{-3}$ ($r_0 = 1.14 \text{ fm}$), $b_v = 16 \text{ MeV}$, $b_s = 18 \text{ MeV}$, $K = 220 \text{ MeV}$, $b_{\text{sym}} = 60 \text{ MeV}$.

The surface part of the LDM stiffness C_{LD} of Eqs. (18), (19) was completed by the Coulomb term [5, 31] and surface corrections in the TF1 (thick rare dashed) approximation. The additional surface $A^{-1/3}$

corrections originate mainly from Eqs. (14) as well as in the particle density [26, 29, 30], and $A^{-2/3}$ contributions of $C_{\text{LD}}/\kappa_{\text{LD}}$ into Eqs. (4), see also Eqs. (15). They both improve the comparison presented in Fig. 1. As expected, the surface corrections are more important for smaller particle numbers A while the Coulomb term of the stiffness becomes more significant at larger A , see [26].

However, Fig. 1 displays also obvious importance of other contributions, first of all arising from the shell effects pronounced especially for the quadrupole case, see the top of Fig. 1. They are certainly beyond the smooth TF approximation (18), (12) - (16). The pairing effects in calculations of the inertia within the cranking model [38, 2] lead basically to the $A^{-2/3}$ behavior for not too both heavy and light even-even nuclei [37, 32], $\hbar\omega_2 \approx 30A^{-2/3}$ MeV, $\hbar\omega_3 \approx 50A^{-2/3}$ MeV, shown by dots in Fig. 1. Notice, the mean vibration energy, $\hbar\omega_L$, as function of its multipolarity L , Eqs. (18) and (19), differs essentially from that predicted by the LDM [5], $\hbar\omega_L \propto \sqrt{(L-1)(L+2)L}$, and obtained from the pairing cranking model (PCM) [38], $\hbar\omega_L \propto \sqrt{(L-1)(L+2)/(2L+1)}$, with the same surface LDM stiffness because of different evaluations of the inertia M . As seen from Fig. 1, our TF1 approximation is in rather good agreement with the average of experimental data for all spherical-like (even-even) nuclei, except for the observed enhancement due to the obviously pronounced shell effects in a few double-magic nuclei.

The smooth reduced friction, γ/M , or the dissipation coefficient, is used for analysis of some experimental data on fission, for instance, fission probabilities and pre-scission neutron multiplicities [23 - 25]. It can be approximated analytically as γ_{wf}/M_1 by using Eqs. (4), (12), (15) and (16) ($M \approx M_1$). Up to small corrections, like in the derivation of Eqs. (16) - (19) one obtains

$$\frac{\gamma}{M} \approx -\frac{\kappa_{\text{LD}}}{\gamma_{\text{wf}}} = \frac{32\pi b_v K}{225\hbar b_s (k_F r_0)^4}. \quad (20)$$

This reduced friction, $\gamma_{\text{TF}}/M_{\text{TF}}$, is almost independent of the particle number A and vibration multipolarity L , $\gamma_{\text{TF}}/M_{\text{TF}} \approx 10^{22} \text{ s}^{-1}$ for nuclear parameters mentioned above. Note that it is within the order of evaluations found for explanation of the experimental fission data, $\gamma/M \approx (2 \div 30) \cdot 10^{21} \text{ s}^{-1}$, see Fig. 12 and comments in [24]. We have to point out however that smaller values of the reduced friction correspond to spherical-like shapes and our TF approximation disregards shell effects for high enough temperatures.

In addition, it is convenient to analyze the effective damping coefficient, $\eta = \gamma/2\sqrt{MC}$, as a measure of the effective friction [6]. For this coefficient, the same approximations (12)-(16), like in the derivations (18) - (20), result in

$$\eta \approx \frac{\gamma_{\text{wf}}}{2\sqrt{M_1 C_{\text{LD}}}} = \frac{2A^{1/3}}{15b_s} \sqrt{\frac{2b_v K}{(L-1)(L+2)}}. \quad (21)$$

According to this equation, the quadrupole ($L=2$) collective motion is mainly overdamped, $\eta > 1$, for larger particle numbers, $\eta = 1.1 \div 2.1$ at $A \approx 40 \div 300$, in qualitative agreement with the experimental data discussed in [23 - 25]. It should be also noted that for the octupole modes we found smaller η , underdamped ($\eta < 1$) motion at smaller particle numbers A and overdamped ($\eta > 1$) one at larger A .

5. Shell Corrections of the Transport Coefficients

For calculations of the quasistatic quantities like the free energy \mathcal{F} and the stiffness C , the SCM [1 - 3] was successfully applied in many works [3, 39, 40]. The basic point of these calculations is the Strutinsky renormalization, similar to the SCM binding and deformation energies of nuclei,

$$\mathcal{F} = \mathcal{F}_{\text{LD}} + \delta\mathcal{F}, \quad \delta\mathcal{F} = \mathcal{F}_{\text{sp}}(T, A) - \mathcal{F}_{\text{sp}}(T, A) = \delta\Omega(T, \lambda) = \Omega_{\text{sp}}(T, \lambda) - \tilde{\Omega}_{\text{sp}}(T, \lambda), \quad (22)$$

where \mathcal{F}_{LD} is the LDM free energy, $\mathcal{F}_{\text{sp}}(T, A)$ and $\Omega_{\text{sp}}(T, \lambda)$ are respective the quantum single-particle free energy and the grand thermodynamic potential, $A = 2\sum_i \tilde{n}_i$ [41]. Their SCM averaged quantities $\mathcal{F}_{\text{sp}}(T, A)$

and $\tilde{Q}_{\text{sp}}(T, \lambda)$ and smooth occupation numbers \tilde{n}_i are determined with help of the averaging procedure similar to that explained in [1] (see also the first footnote) but for a given temperature and valid for the averaging parameter Δ under the conditions $T/\varepsilon_F A^{1/3} \ll \Delta \ll k_F R \approx 2A^{1/3}$. The $\delta\mathcal{F}$ and $\delta\Omega$ in Eqs. (22) are the corresponding shell structure components of the SCM. The stiffness C can be then calculated by

$$C = \left(\frac{\partial^2 \mathcal{F}}{\partial Q^2} \right)_{Q=0} = C_{\text{LD}} + \delta C, \quad \delta C = C(0) - \tilde{C}(0), \quad C(0) = \left(\frac{\partial^2 \mathcal{F}_{\text{sp}}}{\partial Q^2} \right)_{Q=0}, \quad (23)$$

where $C(0)$ is the stiffness of the independent particle model, $\tilde{C}(0)$ and δC are its Strutinsky average in $k_F R$ and shell component, respectively. The averaged stiffness $\tilde{C}(0)$, Eqs. (23), can be found with the averaging parameters, $\Delta = 1.5$ and $\mathcal{M} = 3$, for which we found a rather good plateau condition [1 - 3]. Note also that in the calculation of the δC , Eqs. (23), we shall neglect approximately the small curvature of single-particle levels with respect to the dominating contributions of squares of their slopes in Eq. (18) of [39] for finite temperature.

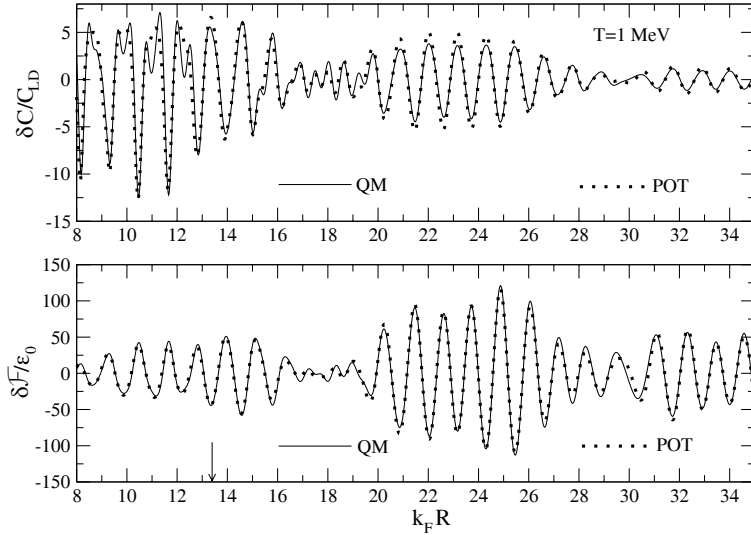


Fig. 2. Free energy, $\delta\mathcal{F}$ (bottom), and quadrupole stiffness, δC (top), shell corrections versus $k_F R$ at temperature $T = 1$ MeV in units of $\varepsilon_0 = \hbar^2/2mR^2$ and C_{LD} , respectively; QM (Eqs. (22), (23)) and POT (Eqs. (24)) are calculated as explained in the text; $\Delta = 1.5$ and $\mathcal{M} = 3$; the arrow shows $k_F R = 13.36$; the parameters r_0 and b_s are the same as in Fig. 1.

Fig. 2 shows good agreement between the quantum-mechanical (QM) shell corrections $\delta\mathcal{F}$, Eqs. (22), to the free energy \mathcal{F} (see bottom) as well as δC , Eqs. (23), to the stiffness C (top) for the spherical box and the corresponding semiclassical POT results, $\delta\mathcal{F}_{\text{POT}}$ and δC_{POT} , as functions of $k_F R$ at temperature $T = 1$ MeV as example,

$$\delta\mathcal{F}_{\text{POT}} = \sum_{\beta} \delta\mathcal{F}_{\beta}, \quad \delta C_{\text{POT}} = \left(\frac{\partial^2 \delta\mathcal{F}_{\text{POT}}}{\partial Q^2} \right)_{Q=0} = -\frac{5}{84\pi} \sum_{\beta} (k_F L_{\beta})^2 \delta\mathcal{F}_{\beta} \approx -\frac{5}{84\pi} (k_F \bar{L})^2 \delta\mathcal{F}_{\text{POT}}, \quad (24)$$

$$\delta\mathcal{F}_{\beta} = \left(\frac{2\varepsilon_F}{k_F L_{\beta}} \right)^2 \Phi \left(\frac{\pi k_F L_{\beta} T}{2\varepsilon_F} \right) \delta g_{\text{osc}}^{(\beta)}(\lambda), \quad \Phi(\tau) = \frac{\tau}{\sinh(\tau)}. \quad (25)$$

Here, the sums are taken over the periodic orbits β in the spherical cavity, and $\delta g_{\text{osc}}^{(\beta)}(\varepsilon)$ is the β -component of the oscillating part of level density, $g_{\text{osc}}(\varepsilon) = \sum_{\beta} g_{\text{osc}}^{(\beta)}(\varepsilon)$, derived in [10, 11]. In order to obtain the stiffness shell correction, δC_{POT} , in Eqs. (24) we used more general POT sum of Eqs. (24), (25) for $\delta\mathcal{F}_{\text{POT}}$ over periodic orbits β in the slightly deformed spheroidal box potential, which is a good

approximation for the quadrupole ($L=2$) shapes at small quadrupole deformations $Q^{(0)}$. As shown in [7], the Q -derivatives of the strong oscillating cosine in the level density component $\delta g_{\text{osc}}^{(\beta)}(\lambda)$ yield the semiclassically leading contribution of main orbits (triangles, rhomboids and so on) in the meridian plane of spheroidal cavity at these deformations.

The convergence of the POT sum for the stiffness δC_{POT} is more slow than that for the free energy $\delta \mathcal{F}_{\text{POT}}$ because of the additional factor of L_β^2 in δC_{POT} , see Eqs. (24). This convergence is provided by the temperature-damping exponential factor, $\Phi(\pi k_F L_\beta T / 2\varepsilon_F)$, written explicitly in Eq. (25) for $\delta \mathcal{F}_\beta$. The shell corrections $\delta \mathcal{F}_\beta$ to the free energy $\delta \mathcal{F}_{\text{POT}}$, Eqs. (24), decrease exponentially with growing both temperature T and parameter $k_F L_\beta$ due to this factor. Therefore, for large enough temperature and particle numbers, $k_F L_\beta \propto k_F R \sim 2A^{1/3}$, the shortest orbits with average length \bar{L} give the major contribution into the POT sums (24) for $\delta \mathcal{F}_{\text{POT}}$ and δC_{POT} , and approximately, $\delta C \propto -\delta \mathcal{F}$, as shown in (24) and seen in Fig. 2.

In close analogy with the nuclear SCM relationships (22), (23) for the free energy \mathcal{F} and stiffness C , according to Eq. (6), one may obtain the renormalized SCM inertia,

$$M = M_{\text{TF}} + \delta M, \quad \delta M = M(0) - \tilde{M}(0) = 2\hbar^2 \sum_{ij}' \frac{\delta n_i - \delta n_j}{(\varepsilon_j - \varepsilon_i)^3} |\langle i | \hat{F} | j \rangle|^2, \quad (26)$$

where $\delta n_i = n_i - \tilde{n}_i$. In order to compute the averaged QM ‘‘intrinsic’’ inertia $\tilde{M}(0)$ (AQM) as function of $k_F R$ (or particle numbers A , according to Eq. (14)) we note that the only occupation numbers n_i in Eq. (6) depend on the Fermi energy ε_F . Therefore, we may apply the Strutinsky averaging procedure [1 - 3] to the occupation numbers n_i in Eq. (6) by making use of the averaging function, $f_{\text{av}}^{(2\mathcal{M})}[(y_F - y_F)/\Delta]$, $y_F = k_F R$, having the Gaussian weight function with the width parameter Δ and correction polynomial degree of $2\mathcal{M}$ with respect to the y_F variable, see the first footnote. The averaging parameters around $\Delta=4$ and $\mathcal{M}=3$ can be found from study of the plateau condition.

Note that for the friction (at a finite dissipative width Γ depending generally speaking on quantum numbers in Eqs. (5)) a renormalization procedure, similar to Eqs. (26) for the inertia, is assumed to be applied too, $\gamma = \gamma_{\text{TF}} + \delta\gamma$ with $\delta\gamma = \gamma(0) - \tilde{\gamma}(0)$ ($\gamma = \gamma_{\text{TF}}$ in the case $\Gamma=0$). Such theoretical scheme for the stiffness, inertia and friction looks logically more closed and consequent for the *densed* Fermi systems with strong interacting particles because the only quasiparticle states near the Fermi surface should be mainly involved in the calculations based on the one-body Green function representation of Eqs. (5) within the Migdal theory [4]. Other contributions of the single-particle states far from the Fermi surface should be replaced by another, macroscopic (almost local) part of a many-body nature beyond this representation. The macroscopic part is available at the present moment with using phenomenological (experimentally known) properties of nuclei like the particle density of nuclear matter, surface tension, separation energy per one nucleon, incompressibility and so on, similarly to the extended TF approach of Section 4. Note also that other versions of the phenomenological macroscopic components of the friction and inertia can be also considered for the specific dynamical problems. However, as well known [5, 6, 19, 27], the simultaneous use of the irrotational-flow inertia and standard hydrodynamical friction disagrees with experimental data on the nuclear collective excitation energies and fission in many aspects, and the extended TF approach might be preferable for such cases.

6. Comparison of Semiclassical and Quantum Approaches

We now compare the semiclassical quadrupole TF inertia M_{TF} , Eqs. (4), (12), (13), (15), with the corresponding quantum (QM) result (4), (6) as functions of $k_F R$ in Fig. 3. For convenience, this comparison is performed in the irrotational flow units, M_{irr} , with account of the extended TF relationship (14) between the particle number A and $k_F R$. Note that for the perfect Fermi gas in the infinitely deep spherical square-well potential, the static susceptibility $\chi(0)$ is infinity and $M = M(0)$, in contrast to the LDM approach, $\chi_{\text{LD}}(0) = -\kappa_{\text{LD}} - C_{\text{LD}}$, see Eqs. (2), (15).

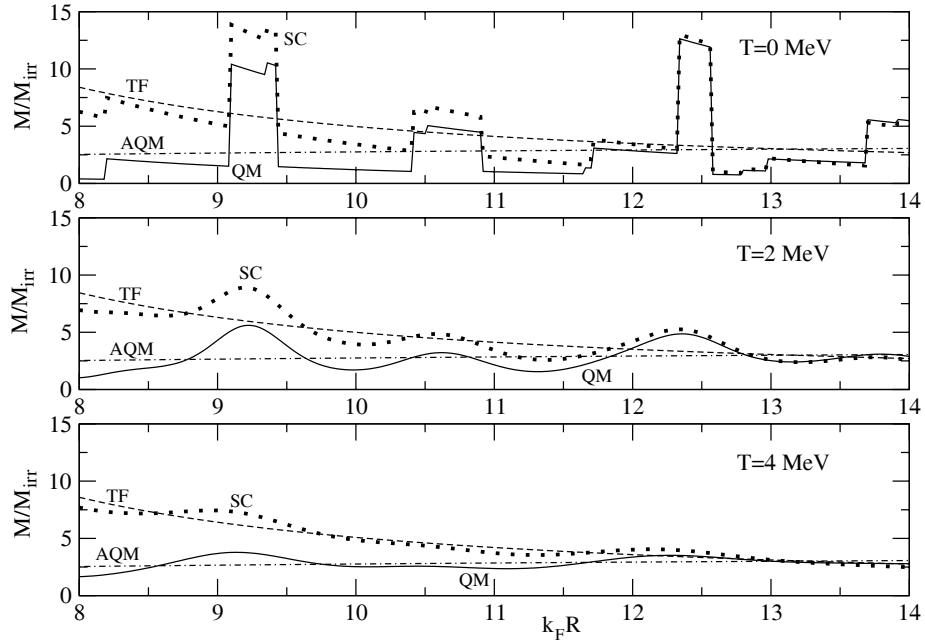


Fig. 3. Inertia M (4) in units of the irrotational flow M_{irr} versus $k_F R$; QM and AQM are the quantum cranking-model results (6) for $M = M(0)$ and its average $\tilde{M}(0)$, respectively; SC is the renormalized inertia (26); TF is the full Thomas - Fermi approach (16); $\Delta = 4$ and $\mathcal{M} = 3$; other parameters are the same as in Figs. 1 and 2.

As seen from Fig. 3, for large enough $k_F R$ and temperatures T , one finds rather close TF values M_{TF} of the inertia (dashed), Eqs. (4), (12), (13), (15), as compared to that of the quantum cranking model (QM) $M(0)$ (solid), Eq. (6), and its average (AQM) $\tilde{M}(0)$ (dash-dotted) defined in Section 5. Notice, the SC inertia (dots) (26) approximately coincides with the QM results near $k_F R \approx 12 \div 14$ ($A \approx 180 \div 300$). However, the $k_F R$ (or particle number $A^{1/3}$) dependence of our smooth TF inertia approach, $M_{\text{TF}} \propto (k_F R)^4$, see discussion of the previous section nearby Eqs. (17), differs from behavior of the irrotational flow inertia, $M_{\text{irr}} \propto (k_F R)^5$, as well as from a little stronger AQM one, which looks as M_{irr} multiplied by $\ln(k_F R)$ at larger $k_F R$.

The most pronounced shell effects, which can be measured by the deviation of the SC from the TF, are seen well in Fig. 3 at zero temperature T for all $k_F R$. The shell oscillation amplitude of the inertia M decreases significantly with increasing temperature T , and practically disappears at $T = 3 \div 4$ MeV.

Fig. 4 displays the semiclassical quadrupole collective friction γ , Eqs. (4), (12), (15), the inertia M , see also Eq. (13), and the free-energy shell corrections $\delta \mathcal{F}$, Eqs. (24), versus the corresponding QM results, $\gamma = 0$, Eqs. (6) and (22) as well as the SC approximation for M , Eqs. (26) (in the middle $\mathcal{F}(k_F R)$ (22) and (24) at $T = 0$). It is example of the completely closed shells related to a large enough magic-particle number $A = 254$ through Eq. (14) for the relationship A to $k_F R$ at zero temperature in the considered spherical box potential. Within the temperature interval restricted by small parameter $(T/\varepsilon_F)^2$ of the Sommerfeld expansion, we may neglect a change of $k_F R$ with temperature for a given particle number A .

The TF friction γ_{TF} (thin frequent dashed, see Eqs. (4), (12), (15)) is shown at the top of Fig. 4. It is a slightly increasing function of temperature T , being typical for the Fermi gas system, and therefore, essentially different from the well-known hydrodynamic collisional decrease with T [6, 19, 27, 28], see the comments after Eq. (14). The TF0 approximation (thick rare dash-dotted) for the “intrinsic” friction $\gamma_{\text{TF}}(0)$, Eqs. (12), is rather close to the temperature-dependent wall formula WF (thick solid) of the local approximation [19, 16]. The latter is equal approximately (up to small T^2 corrections) to the constant γ_{wf} in Eqs. (12). A small difference between the full TF approach for γ_{TF} , Eqs. (4), and the “intrinsic” TF0 approximation, $\gamma_{\text{TF}}(0)$, Eqs. (12) (or the wall formula γ_{wf} in Eqs. (12), $\gamma_{\text{TF}}(0) \approx \gamma_{\text{wf}}$), is due to the relatively small collective consistent corrections, $\sim 2C_{\text{LD}}/\kappa_{\text{LD}}$, see Section 4. However, we have to point out that there

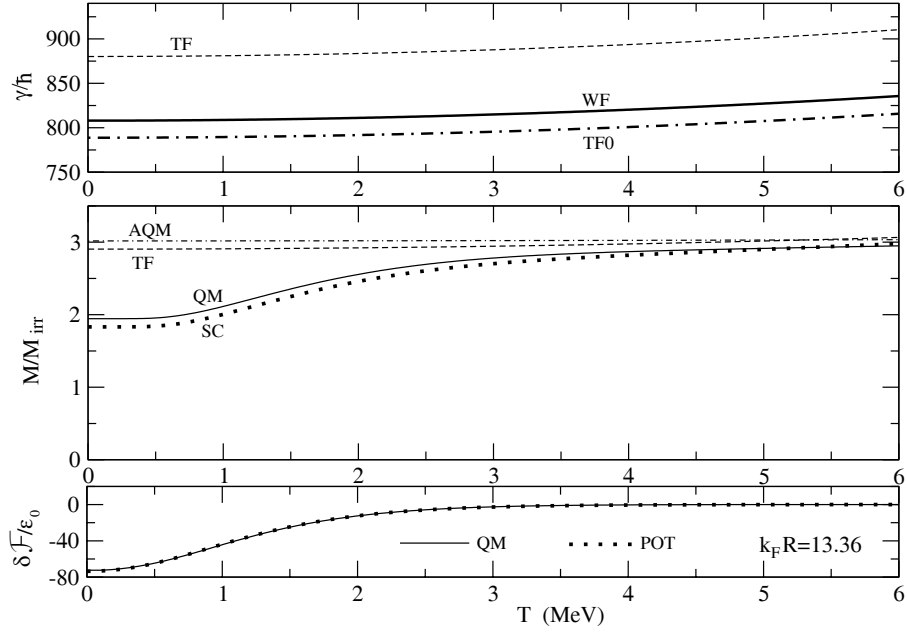


Fig. 4. Friction γ , inertia M and free-energy shell corrections $\delta\mathcal{F}$ versus temperature T at $k_F R = 13.36$ ($A = 254$ through Eq. (14)) in units of \hbar , irrotational flow value M_{irr} and $\varepsilon_0 = \hbar^2/2mR^2$ respectively. *top*: TF is full extended Thomas - Fermi approach (4), (12), (15) for the friction; WF shows its local part (wall-formula); TF0 is the TF approach (12) for $\gamma(0)$; *middle*: QM is the quantum cranking model inertia $M(0)$ (6), AQM its average $\tilde{M}(0)$; SC is renormalized inertia (26); TF is full extended TF approach (16) for the inertia; *bottom*: the free-energy shell corrections the QM $\delta\mathcal{F}$ (22) and $\delta\mathcal{F}_{\text{POT}}$ (24); the parameters are the same as in Figs. 1 - 3.

is a dramatical discrepancy between the finite friction γ_{TF} , Eqs. (4), (12), (15), in the *statistical* TF approach and its *zero* QM values of the *perfect Fermi-gas* cranking model at $\Gamma = +0$. The reason is a renormalization procedure, similar to the replace of the averaged QM free energy \mathcal{F}_{sp} , stiffness $\tilde{C}(0)$ and inertia $\tilde{M}(0)$, of the independent single-particle model, see Eqs. (22), (23) and (26) by the corresponding phenomenological quantities \mathcal{F}_{LD} , C_{LD} of the LDM and M_{TF} of the extended TF approach with the SCM for a densed Fermi system.

In the bottom of Fig. 4, one finds perfect agreement between the QM, Eqs. (22), and the POT, Eqs. (24), temperature dependences of the free-energy shell corrections $\delta\mathcal{F}$. A similar sharp decrease of the both quantum shell corrections in the free energy, Eqs. (22), and the inertia, Eqs. (26), at about the same temperature T_{cr} , are seen from comparison of the bottom and middle panels of this Figure. The reason is that the corresponding POT sums for δM (see [7, 8]) and $\delta\mathcal{F}$, Eqs. (24), decrease exponentially with increasing temperature T and semiclassical parameter $k_F L_\beta$ due to the same temperature damping factor, $\Phi(\pi k_F L_\beta T / 2\varepsilon_F)$, shown in Eqs. (25) for $\delta\mathcal{F}_\beta$.

The middle panel of Fig.4 transparently shows that the SC inertia (dots) rapidly converges to the TF asymptotics for temperatures $T \gtrsim T_{\text{cr}} = 2 \div 3$ MeV, where T_{cr} is the critical value for disappearance of $\delta\mathcal{F}$ (see Eqs. (22), (24)). The TF and SC inertias depend on the incompressibility modulus K . For its conventional nuclear value, $K = 220$ MeV, we obtain a rather good agreement of the TF approximation versus QM (also its average AQM, thin frequent dash-dotted) and SC for particle numbers $A \sim 180 \div 300$ and temperatures $T \gtrsim T_{\text{cr}}$, see the middle of Fig. 4, and Fig. 3 nearby $k_F R \sim 12 \div 14$ at $T \sim > 2$ MeV. This agreement becomes the better the larger temperature T , as shown in Fig. 4 for example at $k_F R = 13.36$. The magnitudes of the QM (AQM), SC and its TF asymptotic inertias, M , for high enough temperatures, $T \gtrsim T_{\text{cr}}$, are a factor of about 3 larger than the irrotational flow value M_{irr} . As seen from the deflection of the SC from the TF inertia in the middle of Fig. 4, the shell effects are rather strong for temperatures smaller than T_{cr} . In the zero-temperature limit we found a minimum of about $2M_{\text{irr}}$ in the QM and SC inertias M . Such a decrease might be related to a magic particle number with the closed shells.

Fig. 5 compares the temperature dependences of the quadrupole collective excitation energies, $\hbar\sqrt{C/M}$, reduced friction, γ/M , and effective friction, $\eta = \gamma/2\sqrt{CM}$, for the TF approximation versus the SC and QM results at $\Gamma \rightarrow +0$, except for obvious QM zeros of the quantities proportional to γ . All quantities in Fig. 5 are rather slow functions of temperature T at large enough values, $T \gtrsim T_{cr}$. As expected, the critical temperature for disappearance of the shell effects in all these quantities is near T_{cr} like in Fig. 4 for the inertia, δM , and the free energy, $\delta \mathcal{F}$, as well as for the stiffness, δC , shell corrections. For temperatures $T \gtrsim T_{cr}$, the SC practically coincides with its almost constant TF asymptotics, according to Eqs. (22) - (26). The significant shell effects are manifested at temperatures smaller than T .

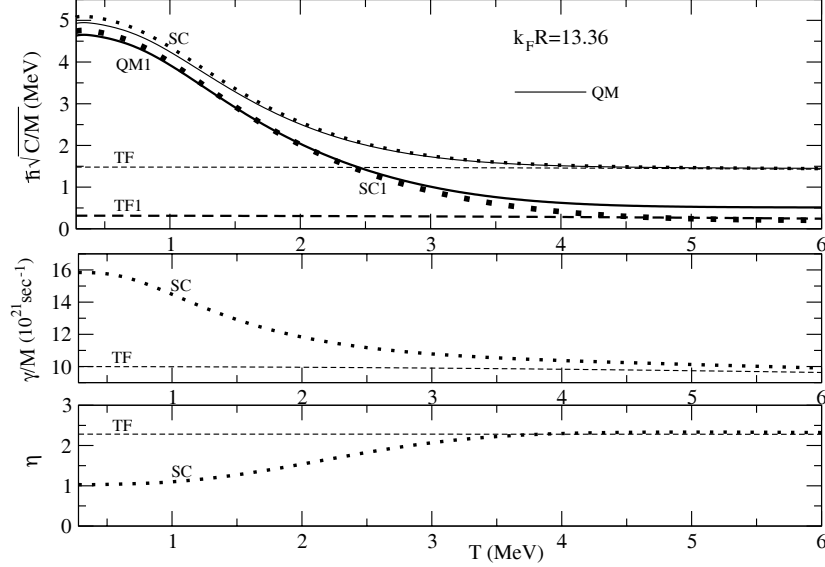


Fig. 5. Collective quadrupole vibration energy $\hbar\sqrt{C/M}$, reduced friction γ/M , and effective friction $\eta = \gamma/2\sqrt{MC}$ parameters versus temperature T ; *top*: TF and SC are given by Eq. (18) with the stiffness C_{LD} (4), (15), inertia M_{TF} (16) and the renormalized quantum stiffness (23), inertia (26), respectively; QM1 and TF1 are the QM and TF approach but with the including Coulomb and surface corrections as explained in the text; SC1 is the corresponding renormalized quantity (18), (23), (26); *middle*: TF and SC show Eq. (20) with the inertia M_{TF} and the renormalized quantum inertia (26); the friction γ_{TF} is given by Eqs. (4), (12), (15); *bottom*: the same TF and SC approaches for η (21) as in the top and middle, see captures of Figs. 1 - 4 for the parameters.

As shown in the top panel of Fig. 5, the QM (thin solid) and SC (dots) vibration energy parameter, $\hbar\sqrt{C/M}$, is well approximated by the TF curve (thin frequent dashed) at temperatures $T \gtrsim T_{cr}$, where the shell effects are exponentially small. Such a parameter at finite temperature might be used in analysis of fission experimental data [23 - 25]. Again, a good agreement between QM and SC energies, $\hbar\sqrt{C/M}$, can be found for all temperatures. It is similar to the results obtained for the inertia, see Fig. 4, because of the same renormalized stiffness C used in both QM and SC calculations, and the only inertia M is critical in this comparison. We note the significant shell enhancement in the collective vibration energies, $\hbar\sqrt{C/M}$, at smaller temperatures which improves comparison with the experimental results for quadrupole collective states in magic cold nuclei, as seen in Fig. 1. These energies in the small temperature limit are increased due to the minimum of the inertia, δM , and maximum of the stiffness, δC , associated both with the minimum of the free energy, $\delta \mathcal{F}$, shell corrections for a magic particle number. A small decrease of the vibration energy maximum at low temperatures, see the QM1 (thick solid) for the quantum result and its SC1 (full heavy rare squares) renormalization with the TF1 smooth high temperature asymptotics (thick rare dashed) in this part of Fig. 5, is related mainly to the negative Coulomb stiffness correction rather than with the surface corrections (both are included in QM1, TF1 and SC1 like in Fig. 1) because of a large particle number. It should be noted however that the comparison of our SC results with experimental data for magic

nuclei, as shown, for instance for Pb^{208} in Fig. 1, requires certainly more realistic calculations [5, 6]. On a qualitative level, we may only point out here that our SC results become more close to the experimental data for magic nuclei mainly due to the account for shell effects.

As seen in the middle panel of Fig. 5, for higher temperatures the TF reduced friction, γ/M , is of the order of the estimations given in Section 4, which are comparable roughly within the order with its evaluations from experimental fission data in Fig. 12 of [24] for nearly spherical shapes. More exact SC values are notably enhanced at smaller temperatures due to the shell effects. Note that the maximum of γ/M at zero temperature can be explained by a minimum of the both free energy \mathcal{F} and inertia M , see Fig. 4, because there is no friction shell corrections at zero dissipation $\Gamma = 0$, $\gamma = \gamma_{\text{TF}}$ within the SC approach. In this comparison, we should take into account that the Thomas - Fermi approach is expected to be a good approximation, at least, for enough heated systems, for which we may disregard shell effects. We neglected also the nuclear equilibrium deformations, which influence essentially on the reduced friction for fission processes, see the corresponding comments in [12, 23 - 25]. We should expect also importance of the residue interactions like two-body collisions in this comparison.

A rather strong overdamped motion, $\eta > 1$, at temperatures $T \gtrsim T_{\text{cr}}$, where the SC practically coincides with the TF approximation, is shown in the bottom panel of this Figure. As seen from comparison of the TF versus the SC, the effective friction η is monotonically decreasing to about one with decrease of temperature because of the shell effects. These calculations are also roughly in agreement with evaluations of the effective damping coefficient η from experimental data on fission, see Fig. 12 in [24].

Thus, our results for the collective vibration energies at zero temperature and the reduced and effective friction coefficients for larger temperatures are qualitatively in reasonable agreement with experimental data discussed in [20 - 25].

7. Conclusions

For low-lying nuclear collective excitations, within the lowest orders of the POT in \hbar , corresponding to the extended Thomas - Fermi approximation, we derived smooth friction and inertia for multipole vibrations near the spherical shape of the infinitely deep spherical square-well potential. The averaged semiclassical friction is the wall (local) formula modified however, by small non-local corrections depending on the vibration multipolarity. It is shown due to the consistency relation between the potential and density variations that the collective TF inertia, M_{TF} , is smaller in order of the semiclassical parameter, $k_F R \sim A^{1/3}$, as compared to the inertia of irrotational flow M_{irr} . However, this consistent inertia is in fact significantly larger than M_{irr} of the LDM because of a difference in coefficients. The smooth collective inertia, M_{TF} , is basically proportional to the surface energy constant b_s , like the stiffness coefficient, C_{LD} , as well as the LDM coupling constant, $\kappa_{\text{LD}}^{-1} \propto b_s$. In this sense, they all describe the nuclear surface modes. The smooth collective inertia M_{TF} and friction γ_{TF} are slightly increasing functions of temperature due to the small quadratic corrections in contrast to their hydrodynamical behavior.

Up to the shell effects, we found that the statistically averaged low-lying collective vibration energies in spherical nuclei can be approximated largely by the $A^{-1/3}$ particle-number dependence at zero temperature for heavy enough nuclei, unlike their $A^{-1/2}$ function predicted by the liquid-drop model. As the TF inertia M is significantly larger than that for irrotational flow M_{irr} , our vibration energies are in better agreement with their mean experimental data as compared to the standard hydrodynamical results. We point out importance of the shell effects for magic particle numbers as well as the Coulomb interaction in sufficiently heavy nuclei, especially for the quadrupole collective vibration modes.

Our semiclassical results for the reduced and the effective friction coefficients are in agreement on a qualitative level with some experimental fission data. The consistent TF approach can be also used for calculations of the smooth parts of transport coefficients, similarly as in the SCM. We pointed out importance of the renormalization procedure for the inertia, like for the shell correction calculations of the nuclear free energy and stiffness. According to the POT, the shell structure components δM for the inertia and δC for the stiffness exponentially disappear approximately at about the same temperatures $2 \div 3$ MeV as for the free-energy shell corrections $\delta \mathcal{F}$, and the SC and TF values practically coincide for larger temperatures. After the SCM renormalization of the quantum transport coefficients, we obtained better

results toward experimental data for the quadrupole vibration excitation energy at zero temperature, and for the reduced friction and effective damping parameters at larger temperatures, as compared to the hydrodynamical model. The SCM (quantum and semiclassical) calculations of the transport coefficients might be helpful for understanding and overcoming some problems within the linear response theory at finite two-body dissipation related to a residue interaction.

We thank H. Hofmann, F. A. Ivanyuk, V. M. Kolomietz, V. A. Plujko, V. Yu. Denisov, V. I. Abrosimov, V. P. Aleshin, P. Schuck, O. M. Gorbachenko and A. I. Sanzhur for many fruitful discussions and suggestions. The authors gratefully acknowledge F. A. Ivanyuk for his code of the quantum calculations, also V. A. Plujko and O. M. Gorbachenko for providing the files with experimental data on the low-lying vibration energies, which are prepared in accordance with [20, 21]. One of us (A. G. M.) acknowledges also Deutsche Forschungsgemeinschaft for partial financial support of this work and the Physical Department of the Technical Munich University for very kind hospitality during his stay at Garching.

REFERENCES

1. *Strutinsky V.M.* // Nucl. Phys. - 1967. - Vol. A95. - P. 420; Ibid. - 1968. - Vol. A 22. - P. 1.
2. *Brack M., Damgard L., Jensen A.S. et al.* // Rev. Mod. Phys. - 1972. - Vol. 44. - P. 320.
3. *Brack M., Bhaduri R.K.* Semiclassical Physics. Frontiers in Physics. - 1997. - Vol. 96. - Addison-Wesley, Reading, MA.; 2nd edition. - Westview Press, Boulder - 2003.
4. *Migdal A.B.* Theory of finite Fermi systems and applications to the atomic nuclei. - N.-Y.: Wiley, 1967; New edition in Russian. - 1983.
5. *Bohr A., Mottelson B.* Nuclear structure. - Vol. 2 - N.-Y.: Benjamin Inc., 1975.
6. *Hofmann H.* // Phys. Rep. - 1997. - Vol. 284. - P. 137.
7. *Magner A.G., Vydrug-Vlasenko S.M., Hofmann H.* // Nucl. Phys. - 1991. - Vol. A524. - P. 31.
8. *Magner A.G., Gzhebinsky A.M., Fedotkin S.N.* // Scientific Papers of the Institute for Nuclear Research. - 2005. - Vol. 1(14). - P. 7.
9. *Gutzwiller M.* // J. Math. Phys. - 1971. - Vol. 12. - P. 343; Chaos in Classical and Quantum Mechanics. - N.-Y.: Springer-Verlag, 1990.
10. *Balian R.B., Bloch C.* // Ann. Phys. - 1972. - Vol. 69. - P. 76.
11. *Strutinsky V.M.* // Nukleonika. - 1975. - Vol. 20. - P. 679; *Strutinsky V.M., Magner A.G.* // Sov. Phys. Part. Nucl. - 1976. - Vol. 7. - P. 138.
12. *Ivanyuk F.A., Hofmann H., Pashkevich V.V., Yamaji J.* // Phys. Rev. - 1997. - Vol. C55. - P. 1730.
13. *Blocki J., Bonch Y., Nix J.R., Swiatecki W.J.* // Ann. of Phys. (N.-Y.) - 1978. - Vol. 113. - P. 330.
14. *Koonin S.E., Randrup J.* // Nucl. Phys. - 1977. - Vol. A289. - P. 475.
15. *Balian R., Bloch C.* // Ann. of Phys. (N.-Y.) - 1970. - Vol. 60. - P. 401; Ibid. - 1971. - Vol. 63. - P. 592.
16. *Koonin S.E., Hatch R.L., Randrup J.* // Nucl. Phys. - 1977. - Vol. A283. - P. 87.
17. *Kolomietz V.M.* // Bull. Acad. Sci. of the USSR. - 1978. - Vol. 42. - P. 49; Sov. Journ. Nucl. Phys. - 1978. - Vol. 28. - P. 186.
18. *Yannouleas C., Broglia R.A.* // Ann. of Phys. (N.-Y.) - 1992. - Vol. 217. - P. 105.
19. *Hofmann H., Ivanyuk F.A., Yamaji J.* // Nucl. Phys. - 1996. - Vol. A598. - P. 187.
20. *Raman S., Nestor Jr.C.W., Tikkanen P.* // At. Data Tables. - 2001. - Vol. 78. - P. 1.
21. *Kibedi T., Spear R.H.* // Ibid. - 2005. - Vol. 89. - P. 77.
22. *Handbook for calculations of nuclear reaction data. (Reference Input Parameter Library, RIPL2.)* / Sci. Sec. Oblozhinsky P. and Herman M. - IAEA-TECDOC. April, 2005; <http://www-nds.iaea.org/RIPL-2/>.
23. *Gontchar I.I., Fröbrich P.* // Phys. of Atom. Nucl. - 1994. - Vol. 57. -P. 1181.
24. *Hilsher D., Gontchar I.I., Rossner H.* // Phys. of Atom. Nucl. - 1994. - Vol. 57. - P. 1187.
25. *Fröbrich P., Gontchar I.I.* // Phys.Rep. 1998. - Vol. 292. - P. 131.
26. *Magner A.G., Gzhebinsky A.M., Fedotkin S.N.* // Physics of Atomic Nuclei. - 2006. - Vol. 69. - P. 10 (abstract); 2007 (in press).
27. *Hofmann H., Ivanyuk F.A., Magner A.G.* // Acta Physica Pol. - 1998. - Vol. B29. - P. 375.
28. *Magner A.G., Kolomietz V.M., Hofmann H., Shlomo S.* // Phys. Rev. - 1995. - Vol. C51. - P. 2457.
29. *Strutinsky V.M., Magner A.G., Denisov V.Yu.* // Z. Phys. - 1985. - Vol. A322. - P. 149.
30. *Strutinsky V.M., Magner A.G., Brack M.* // Z. Phys. - 1984. - Vol. A318. - P. 205.
31. *Bohr A., Mottelson B.* Nuclear structure. - Vol. 1. - N.-Y.: Benjamin Inc., 1971.
32. *Plujko V.A.* Theory of nuclei and nuclear processes. Physics of atomic nuclei (in Ukrainian). - Kiev: Edition Center "Kiev University", 2002.
33. *Reinhard P.-G., Bender M., Nazarevich W., Vertse T.* // Phys. Rev. - 2006. - Vol. C73. - P. 014309.
34. *Chabanat E., Bonche P., Haensel P. et al.* // Nucl. Phys. - 1998. - Vol. A635. - P. 231.
35. *Möller P., Nix J.R., Myers W.D., Swiatecki W.J.* // At. Data Nucl.Data Tables. - 1995. - Vol. 59. - P. 185.
36. *Gorielly S., Tondeur F., Pearson J.M.* // Ibid. - 2001. - Vol. 77. - P. 311.

37. *Plujko V.A., Gorbachenko O.M.* // Scientific Papers of the Institute for Nuclear Research. - 2005. - No. 2 (15). - P. 17; *Plujko V.A.* Research Co-ordination Meeting "Parameters for Calculation of Nuclear Reactions of Relevance to Non-energy Nuclear Applications" (RIPL-3), IAEA Headquarters. - Vienna, Austria, 28.11 - 2.12. 2005, report, in press.
38. *Brogli A., Barranco R., Bertsch G.F., Vigezzi E.* // Phys.Rev. - 1993. - Vol. C49. - P. 552.
39. *Hofmann H., Ivanyuk F.A.* // Z. Phys. 1993. - Vol. A344. - P. 285.
40. *Ivanyuk F.A., Hofmann H.* // Nucl. Phys. - 1999. - Vol. A657. - P. 19.
41. *Landau L.D., Lifshits E.M.* // Course of Theoretical Physics. - Vol. 5. Statistical Physics. - N. Y.: Pergamon, 1992. - P. 1.
42. *Hofmann H.* // Phys. Lett. - 1976. - Vol. 61B. - P. 423.

КВАЗИКЛАСИЧЕСКИЕ ТРАНСПОРТНЫЕ СВОЙСТВА И ОБОЛОЧЕЧНАЯ СТРУКТУРА В КОЛЛЕКТИВНОЙ ЯДЕРНОЙ ДИНАМИКЕ

А. Г. Магнер, А. Н. Гжебинский, С. Н. Федоткин

В рамках теории периодических орбит в нижайших порядках квазиклассического разложения, соответствующих расширенному приближению Томаса - Ферми, получены транспортные коэффициенты для низколежащих ядерных коллективных возбуждений. В расчетах рассмотрены мультипольные колебания сферических ядер в приближении среднего поля в виде бесконечно глубокой потенциальной ямы. Показано, что коллективный массовый параметр существенно больше рассчитанного в модели безвихревой жидкости из-за учтенного условия согласования для плотности и потенциала. Гладкие транспортные коэффициенты используются как макроскопический компонент в модифицированном методе оболочечных поправок для описания медленной коллективной динамики. После этой перенормировки квантовая кренкинг-модельная формула для массового параметра согласуется с квазиклассическими результатами для больших значений числа частиц и температуры. Вычисленные усредненные энергии колебаний, приведенное трение и эффективное затухание в достаточно тяжелых ядрах находятся в лучшем согласии с экспериментальными данными, чем используемые в рамках гидродинамической модели.

КВАЗИКЛАСИЧНІ ТРАНСПОРТНІ ВЛАСТИВОСТІ ТА ОБОЛОНКОВА СТРУКТУРА В КОЛЕКТИВНІЙ ЯДЕРНІЙ ДИНАМІЦІ

О. Г. Магнер, А. М. Гжебинський, С. М. Федоткін

У рамках теорії періодичних орбіт у найнижчому порядку квазікласичного розкладу, що відповідає розширеному наближенню Томаса - Фермі, отримано транспортні коефіцієнти для низьколежачих ядерних колективних збуджень. У розрахунках розглянуто мультипольні коливання сферичних ядер у наближенні середнього поля у вигляді нескінченно глибокої потенціальної ями. Показано, що колективний масовий параметр є суттєво більшим, ніж розрахований у моделі безвихревої рідини через враховану умову узгодження для густини та потенціалу. Гладкі транспортні коефіцієнти використовуються як макроскопічний компонент у модифікованому методі оболонкових поправок для опису повільної колективної динаміки. Після цього перенормування квантова кренкинг-модельна формула для масового параметра узгоджується з квазікласичними результатами для великих значень числа частинок і температури. Обчислені усереднені енергії коливань, приведені тертя та ефективне затухання в досить важких ядрах краще узгоджуються з експериментальними даними, ніж обраховані в рамках гідродинамічної моделі.